HHS Public Access
Author manuscript
Proc SPIE Int Soc Opt Eng. Author manuscript; available in PMC 2018 May 17.

Published in final edited form as:
Proc SPIE Int Soc Opt Eng. 2017 February ; 10137: . doi:10.1117/12.2254442.

Brain structure in sagittal craniosynostosis

Beatriz Paniagua[a], **Sunghyung Kim**[b], **Mahmoud Moustapha**[b], **Martin Styner**[b], **Heather Cody-Hazlett**[c], **Rachel Gimple-Smith**[c], **Ashley Rumple**[b], **Joseph Piven**[c], **John Gilmore**[b], **Gary Skolnick**[d], and **Kamlesh Patel**[d]

[a]Kitware Inc., 101 Weaver St Suite G4, Carrboro, NC, United States 27510

[b]University of North Carolina, School of Medicine, Department of Psychiatry, 101 Manning Drive, Chapel Hill, North Carolina 27599, United States

[c]Carolina Institute for Developmental Disabilities, University of North Carolina at Chapel Hill, 100 Renee Lynn Ct, Chapel Hill, North Carolina 27599, United States

[d]Washington University in St. Louis, Department of Plastic and Reconstructive Surgery, School of Medicine 660 South Euclid Ave., St. Louis, Missouri 63110

Abstract

Craniosynostosis, the premature fusion of one or more cranial sutures, leads to grossly abnormal head shapes and pressure elevations within the brain caused by these deformities. To date, accepted treatments for craniosynostosis involve improving surgical skull shape aesthetics. However, the relationship between improved head shape and brain structure after surgery has not been yet established. Typically, clinical standard care involves the collection of diagnostic medical computed tomography (CT) imaging to evaluate the fused sutures and plan the surgical treatment. CT is known to provide very good reconstructions of the hard tissues in the skull but it fails to acquire good soft brain tissue contrast. This study intends to use magnetic resonance imaging to evaluate brain structure in a small dataset of sagittal craniosynostosis patients and thus quantify the effects of surgical intervention in overall brain structure. Very importantly, these effects are to be contrasted with normative shape, volume and brain structure databases. The work presented here wants to address gaps in clinical knowledge in craniosynostosis focusing on understanding the changes in brain volume and shape secondary to surgery, and compare those with normally developing children. This initial pilot study has the potential to add significant quality to the surgical care of a vulnerable patient population in whom we currently have limited understanding of brain developmental outcomes.

Keywords

Full vault reconstructive surgery; sagittal craniosynostosis; Osteoarthritis; Statistical Shape Analysis; Brain Tissue segmentation; Computer Assisted Intervention Planning

1. INTRODUCTION

Craniosynostosis, the premature fusion of one or more cranial sutures, leads to grossly abnormal head shapes and pressure elevations within the brain caused by these deformities[1]. Historically, sagittal synostosis has been the predominant type, occurring in 1 of 5000 births[2,3]. Sagittal craniosynostosis involves an early closure of the sagittal suture. This suture runs front to back, down the middle of the top of the head. This fusion causes a long, narrow skull. The skull is long from front to back and narrow from ear to ear. Sagittal synostosis may be observed in syndromic craniosynostosis, and it might present itself paired with a coronal or lamboid suture synostosis.

To date, accepted treatments for craniosynostosis involve improving surgical skull shape aesthetics[4]. Without medical intervention, these skull shapes persist, and worsen with on-going growth. However, relationships between improved head shape after surgery and other developmental outcomes such as brain structure and shape have not been established.

A current gap in the understanding craniosynostosis is the absence brain structural data that could allow the study of brain before and after surgery, and thus the quantification of any effects of surgical intervention. Also, assumptions are made that improved skull shape leads to normalized brain volume and shape. However, these assumptions must be tested with data that characterize peri-operative brain shape and volume and compare it with normative databases of brain development. Another existing gap is that typically, clinical standard care in craniosynostosis involves the collection of diagnostic medical computed tomography (CT) imaging to evaluate the fused sutures and plan the surgical treatment. CT is known to provide very good reconstructions of the hard tissues in the skull but it fails to acquire good soft brain tissue contrast.

In the work presented in this manuscript we intend to use advanced and validated[5–9] neuroimaging software in an existing magnetic resonance imaging (MRI) dataset[10] to compute structural brain biomarkers in sagittal craniosynostosis patients, and to compare with existing normative databases. Through this work we will determine reliable and reproducible quantitative measures for assessing surgical outcomes and to improve the clinical knowledge on brain structure in craniosynostosis. The ultimate goal of this study is to measure brain structure before and after surgical correction compared with normal developing children, in order to elucidate relationships between fused sutures and brain structure/function.

2. MATERIALS

We used 10 magnetic resonance imaging (MRI) scans obtained from five male pediatric patients (ages ranging between 3-21 months) presenting sagittal synostosis (see figure 1). Imaging data was obtained retrospectively from a dataset collected between 1993 and 2006 at the Washington University of St Louis. Acquisitions were in the sagittal plane using an MPRAGE sequence on a Siemens Magnetom Vision MRI scanner, with the following parameters: matrix 256 × 256, FOV ranging from 20.0 to 25.6 cm, slice thickness −1.0mm, and flip angle = 12°.

The tissue structural data obtained from these craniosynostosis patients was compared to 168 healthy developing, age (range 5.5-28 months) and sex-matched controls (male) from an NIH funded Autism Center for Excellence (ACE) Network project studying infants at-risk for autism and typically developing peers, called the Infant Brain Imaging Study, or IBIS network[11]. Specifically for full brain volume and shape analyses, we also used a small cohort of 37 male neonates (ages ranging 7days to 1 month old) from a bigger neurodevelopment dataset[12] to improve our initial estimation of shape regression.

Images were acquired on a Siemens head-only 3T scanner (Allegra, Siemens Medical System, Erlangen, Germany). Infants were scanned unsedated while asleep, fitted with ear protection and had their heads secured in a vacuum-fixation device. T1-weighted structural pulse sequences were a 3D magnetization prepared rapid gradient echo (MP-RAGE TR = 1820 msec, inversion time = 400 msec, echo time = 4.38 msec, flip angle = 7 degrees, n = 57). Proton density and T2-weighted images were obtained with a turbo spin echo sequence (TSE, TR = 6200 msec, TE1 = 20 msec, TE2 = 119 msec, flip angle 150 degrees). Spatial resolution was 1 × 1 × 1 mm voxel for T1-weighted images, 1.25 × 1.25 × 1.5 mm voxel with 0.5 mm interslice gap for proton density/T2-weight images. These sequences were chosen to optimize signal to noise and allow for efficient tissue segmentation in this age group using minimal scan times to reduce the likelihood of motion during the scan sequence.

3. METHODS

All T1-weighted MR images underwent intensity non-uniformity correction[13], and then rigid registration to stereotaxic space via mutual information using BRAINSFit[14]. The skull was extracted using a majority voting approach using the 9 individual T1 masks. For over 6 month scans, tissue classification via Atlas-Based Classification (ABC)[15] performed an atlas based single modality segmentation of the T1w data into white matter (WM), gray matter (GM), cerebrospinal fluid (CSF), sub-cortical structures and background. Population average templates and corresponding probabilistic brain tissue priors were constructed for the 12-month-old that brain atlas template computed via joint deformable registration that simultaneously minimizes the differences of intensity and transformation from 104 training images from the 12-month-old dataset within the Infant Brain Imaging Study (IBIS)[16]. For below 6-month scans, brain tissues were generated using the propagating tissues from corresponding MRI (over 6 month scan) via deformable registration using ANTs[17].

3.1 Volumetric analysis

Volume is calculated from the obtained label maps and it is quantified on mm^3. Due to the poor myelination happening in infants, we are evaluating three volume based brain biomarkers: Grey Matter (GM) + White Matter (WM) volume, Cerebrospinal fluid (CSF) volume and full intercranial volume. Intracranial volume (ICV) is the sum of the automatic full brain segmentation results for GM, WM, and CSF (ventricles and subarachnoid space) volumes.

3.2 Shape analysis

We performed local shape analysis on the full brain volumes segmentations via the UNC SPHARM-PDM (Spherical HARMonics Point Distribution Models) shape analysis toolbox[7]. The SPHARM-PDM description is a sampled boundary description with object-inherent correspondence that can only represent objects of spherical topology. The input of SPHARM-PDM toolbox is our set of full brain segmentations. These segmentations are first processed to ensure spherical topology and then converted to surface meshes. Next, a spherical parameterization is computed from the surface meshes using an area-preserving, distortion minimizing spherical mapping. Further, the SPHARM description is computed from the mesh and its spherical parameterization. This description is then sampled into triangulated surfaces via an icosahedron. Full brain surfaces are well represented by a subdivision of level 20 resulting in 4002 surface points. When comparing SPHARM-PDM representations to initial surface reconstructions we see that local surface representation error is smaller than 0.1 mm on average, and global representation (volume) estimated differs in less than 0.1%. Alignment of triangulated surfaces was finally performed using rigid body, Generalized Procrustes alignment that iteratively aligns the surfaces to the population mean. By following this set of steps SPHARM-PDM creates a more uniform representation than the one obtained directly from sampling the binary segmentation into triangulated surfaces. It is important mentioning that all SPHARM-PDM triangulated surfaces were strictly quality controlled to ensure the consistency of shape markers across individuals. We used SPHARM-PDM parametric color-coded maps to visually compare each model in the dataset and make sure the correspondence was consistent across all surfaces.

3.3 Shape regression

Due to the need of accurately age-matched controls for the craniosynostosis subjects, calculating the continuous growth evolution of healthy full brain shapes is the starting point for any further analysis. Only healthy subjects that passed the quality control process described in the previous section were used. After quality control our cohort consisted on 196 normal-developing male subjects that we used to generate healthy regressed brain shapes, using a validated acceleration-based shape regression[9]. Shape regression is a tool we use to build a 4D atlas, offering us the opportunity to continuously measure shape properties. Any desired measurement can simply be extracted from the collection of regressed shapes. 350 full brain shapes were obtained between 7 and 852 days of age (time step = 2.42 days). For the individual shape analysis 10 regressed shapes were extracted for comparison with our individual subjects, with a mean age difference of 0.69 days between age-matched healthy matched regressed brain shape and craniosynostosis brain.

4. RESULTS

Figure 2 shows the results we computed for our brain tissue classification for both normative and sagittal synostosis children.

Only by qualitatively checking the scatterplots presented in figure 1.a. we see slightly enlarged full brain volumes, in accordance with existing literature[18]. Figures 1.b. and 1.c. show the different contributions to different tissues to the total ICV. It is important to indicate that WM+GM in patients with sagittal synostosis match normally developing children and CSF is slightly enlarged.

Volume computed from the 4D healthy regression atlas contrasted with the craniosynostosis patients are presented in figure 3.

This figure clearly indicates the enlarged full brain volume in comparison with normal development before surgery for three of the patients. For two of those patients that enlargement normalizes after surgery, whereas for the remaining patient it does not (see figure 3, red arrows). These results indicate that most structural changes between craniosynostosis patients and age-matched healthy subjects decrease in the post-surgical scans, indicating the necessity of craniosynostosis corrective surgery.

Volume changes are intuitive features that explain atrophy or dilation due to illness as illustrated by our results. Shape analysis can provide additional information to that provided by volume alone, by measuring structural changes at specific locations. Shape analysis is especially useful to measure local changes that are not sufficiently reflected in volume measurements, as seen in figure 4.

We showcase shape analysis results to the patients indicated with green and red arrows in figure 3. For these two example cases one (indicated by the red arrows) is an example of a patient for whose ICV does not normalize after surgical correction, whereas the other (indicated by green arrows) is an example for which ICV normalizes compared with the general normal trend.

Figure 4 – left shows shape analysis results for the patient indicated by the red arrows in figure 3. Shape measurements show the magnitude and location of compression and expansion areas compared with the normative brain growth model. This patient shows the characteristic shape features produced by sagittal synostosis, with enlargement of a maximum of 12 mm in the Posterior-Anterior axis and a maximum compression of 9 mm in the Left-Right axis pre-surgically. The brain deformities are improved with surgical correction, but not completely corrected post-surgically.

Figure 4 – right shows shape analysis results for the patient indicated by the green arrows in figure 3. Shape measurements show the magnitude and location of compression and expansion areas compared with the normative brain growth model. This patient displays a different pattern of shape changes, with generalized enlargement before surgery and after surgery. The brain enlargement features are normalized with surgical correction.

5. DISCUSSION

This small pilot study is one of the first ones in studying the complexity of brain structure before and after sagittal synostosis corrective surgery using advanced quantitative neuroimaging methods and MRI imaging data. While our preliminary results agree with existing craniosynostosis literature[18], they have also found other interesting features happening to a small cohort of sagittal synostosis patients. Slightly enlarged CSF fluid is happening before surgery on all of these patients, and though our sample size is small, that suggests possible existing pathology in the CSF structures of the brain. The cerebrospinal fluid system is an important piece of our understanding of healthy brain development and health, and its real function and mechanisms have been recently brought up by recent discoveries[19]. Further studies including analyzing the shape of the lateral ventricles in craniosynostosis might be useful to elucidate the origin of the increased CSF volume.

Lateral ventricle volume is grows between birth and 1 years of age, and decreases between 1 and 2 years of age, possibly due to the closure of the sutures in that period[20,21]. Some studies have also indicated that the structure of lateral ventricles in-utero is predictive of the shape evolution of this brain structure early in life[22]. With all of this in mind it seems the work presented in this manuscript sets an interesting point of discussion and justifies further, more detailed analysis. We have as well quantitatively demonstrated that head shape improves as compared with normally developing children after corrective surgery. This would not have been possible without the existence of complex methods that explore the growth in 3-dimensions of biological shapes[23,24].

In conclusion this work validates the use of neuroimaging and magnetic resonance imaging to improve the current clinical knowledge about craniosynostosis. These pilot results need to be further explored in a study including a larger craniosynostosis cohort.

References

1. Scott JR, Isom CN, Gruss JS, Salemy S, Ellenbogen RG, Avellino A, Birgfeld C, Hopper RA. Symptom outcomes following cranial vault expansion for craniosynostosis in children older than 2 years. Plast Reconstr Surg. 2009; 123(1):289–97. 9. [PubMed: 19116564]
2. Boop, FA., Shewmake, K., Chadduck, WM. Child's Nerv Syst. Vol. 12. Springer-Verlag; 1996. Synostectomy versus complex cranioplasty for the treatment of sagittal synostosis; p. 371-375.
3. Keating RF. Craniosynostosis: diagnosis and management in the new millennium. Pediatr Ann. 1997; 26(10):600–612. [PubMed: 9339461]
4. Nguyen C, Hernandez-Boussard T, Khosla RK, Curtin CM. A national study on craniosynostosis surgical repair. Cleft Palate Craniofac J. 2013; 50(5):555–560. [PubMed: 23030675]
5. Wang J, Vachet C, Rumple A, Gouttard S, Ouziel C, Perrot E, Du G, Huang X, Gerig G, et al. Multi-atlas segmentation of subcortical brain structures via the AutoSeg software pipeline. Front Neuroinform. 2014; 8:7. [PubMed: 24567717]
6. Paniagua B, Emodi O, Hill J, Fishbaugh J, Pimenta LA, Aylward SR, Andinet E, Gerig G, Gilmore J, et al. 3D of Brain Shape and Volume After Cranial Vault Remodeling Surgery for Craniosynostosis Correction in Infants. Proc Soc Photo Opt Instrum Eng. 2013; 8672:86720V.
7. Styner M, Oguz I, Xu S, Brechbühler C, Pantazis D, Levitt JJ, Shenton ME, Gerig G. Framework for the Statistical Shape Analysis of Brain Structures using SPHARM-PDM. Insight J. 2006; (1071):242–250. [PubMed: 21941375]
8. Yushkevich PA, Piven J, Hazlett HC, Smith RG, Ho S, Gee JC, Gerig G. User-guided 3D active contour segmentation of anatomical structures: significantly improved efficiency and reliability. Neuroimage. 2006; 31(3):1116–1128. [PubMed: 16545965]
9. Fishbaugh J, Prastawa M, Gerig G, Durrleman S. GEODESIC REGRESSION OF IMAGE AND SHAPE DATA FOR IMPROVED MODELING OF 4D TRAJECTORIES. Proc IEEE Int Symp Biomed Imaging. 2014; 2014:385–388. [PubMed: 25356192]
10. Aldridge K, Kane AA, Marsh JL, Yan P, Govier D, Richtsmeier JT. Relationship of brain and skull in pre- and postoperative sagittal synostosis. J Anat. 2005; 206(4):373–385. [PubMed: 15817105]
11. Hazlett HC, Gu H, McKinstry RC, Shaw DWW, Botteron KN, Dager SR, Styner M, Vachet C, Gerig G, et al. Brain volume findings in 6-month-old infants at high familial risk for autism. Am J Psychiatry. 2012; 169(6):601–608. [PubMed: 22684595]
12. Gilmore JH, Kang C, Evans DD, Wolfe HM, Smith JK, Lieberman JA, Lin W, Hamer RM, Styner M, et al. Prenatal and neonatal brain structure and white matter maturation in children at high risk for schizophrenia. Am J Psychiatry. 2010; 167(9):1083–1091. [PubMed: 20516153]
13. Sled JG, Zijdenbos AP, Evans AC. A nonparametric method for automatic correction of intensity nonuniformity in MRI data. IEEE Trans Med Imaging. 1998; 17(1):87–97. [PubMed: 9617910]

14. Jonhson H, Harris G, Williams K. BRAINSFit: Mutual Information Registrations of Whole-Brain 3D Images, Using the Insight Toolkit. Insight J (The Insight Journal-2007 July-December). 2007
15. Van Leemput K, Maes F, Vandermeulen D, Suetens P. Automated model-based tissue classification of MR images of the brain. IEEE Trans Med Imaging. 1999; 18(10):897–908. [PubMed: 10628949]
16. Fonov, V., Evans, AC., Botteron, K., Almli, CR., McKinstry, RC., Collins, DL., Brain Development Cooperative Group. Neuroimage. Vol. 54. NIH Public Access; 2011. Unbiased average age-appropriate atlases for pediatric studies; p. 313-327.
17. Avants, BB., Epstein, CL., Grossman, M., Gee, JC. Med Image Anal. Vol. 12. NIH Public Access; 2008. Symmetric diffeomorphic image registration with cross-correlation: evaluating automated labeling of elderly and neurodegenerative brain; p. 26-41.
18. Lee SS, Duncan CC, Knoll BI, Persing JA. Intracranial Compartment Volume Changes in Sagittal Craniosynostosis Patients: Influence of Comprehensive Cranioplasty. Plast Reconstr Surg. 2010; 126(1):187–196. [PubMed: 20595867]
19. Lun, MP., Monuki, ES., Lehtinen, MK. Nat Rev Neurosci. Vol. 16. Nature Research; 2015. Development and functions of the choroid plexus–cerebrospinal fluid system; p. 445-457.
20. Paniagua B, Lyall A, Berger JB, Vachet C, Hamer RM, Woolson S, Lin W, Gilmore J, Styner M. Lateral ventricle morphology analysis via mean latitude axis. Proc Soc Photo Opt Instrum Eng. 2013; 8672
21. Lyall, AE., Woolson, S., Wolfe, HM., Goldman, BD., Reznick, JS., Hamer, RM., Lin, W., Styner, M., Gerig, G., et al. Early Hum Dev. Vol. 88. Elsevier Ltd; 2012. Prenatal isolated mild ventriculomegaly is associated with persistent ventricle enlargement at ages 1 and 2; p. 691-698.
22. Lyall AE, Paniagua B, Zhaohua L, Zhu H, Shi F, Lin W, Shen D, Gilmore JH, Styner M. Longitudinal lateral ventricle morphometry related to prenatal measures as a biomarker of normal development. MICCAI Work. Perinat Paediatr Imaging PaPI. 2012; 2012
23. Fishbaugh J, Prastawa M, Durrleman S, Piven J, Gerig G. Analysis of longitudinal shape variability via subject specific growth modeling. Med Image Comput Comput Assist Interv. 2012; 15(Pt 1): 731–738. [PubMed: 23285617]
24. Fishbaugh J, Prastawa M, Gerig G, Durrleman S. Geodesic shape regression in the framework of currents. Inf Process Med Imaging. 2013; 23:718–729. [PubMed: 24684012]

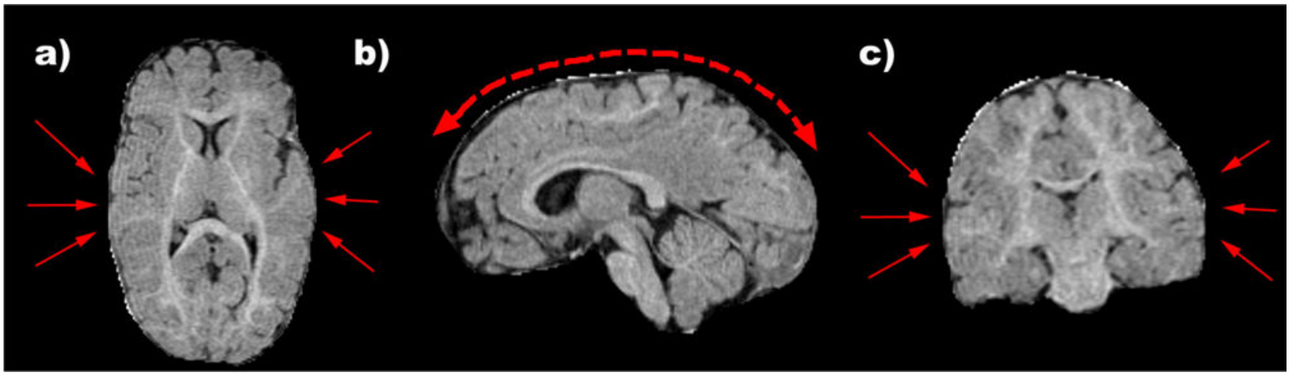

Figure 1.

Example of anatomical features displayed in a male sagittal craniosynostosis subject. Areas of enlargement and compressing are indicated with red arrows in a) axial, b) sagittal and c) coronal views.

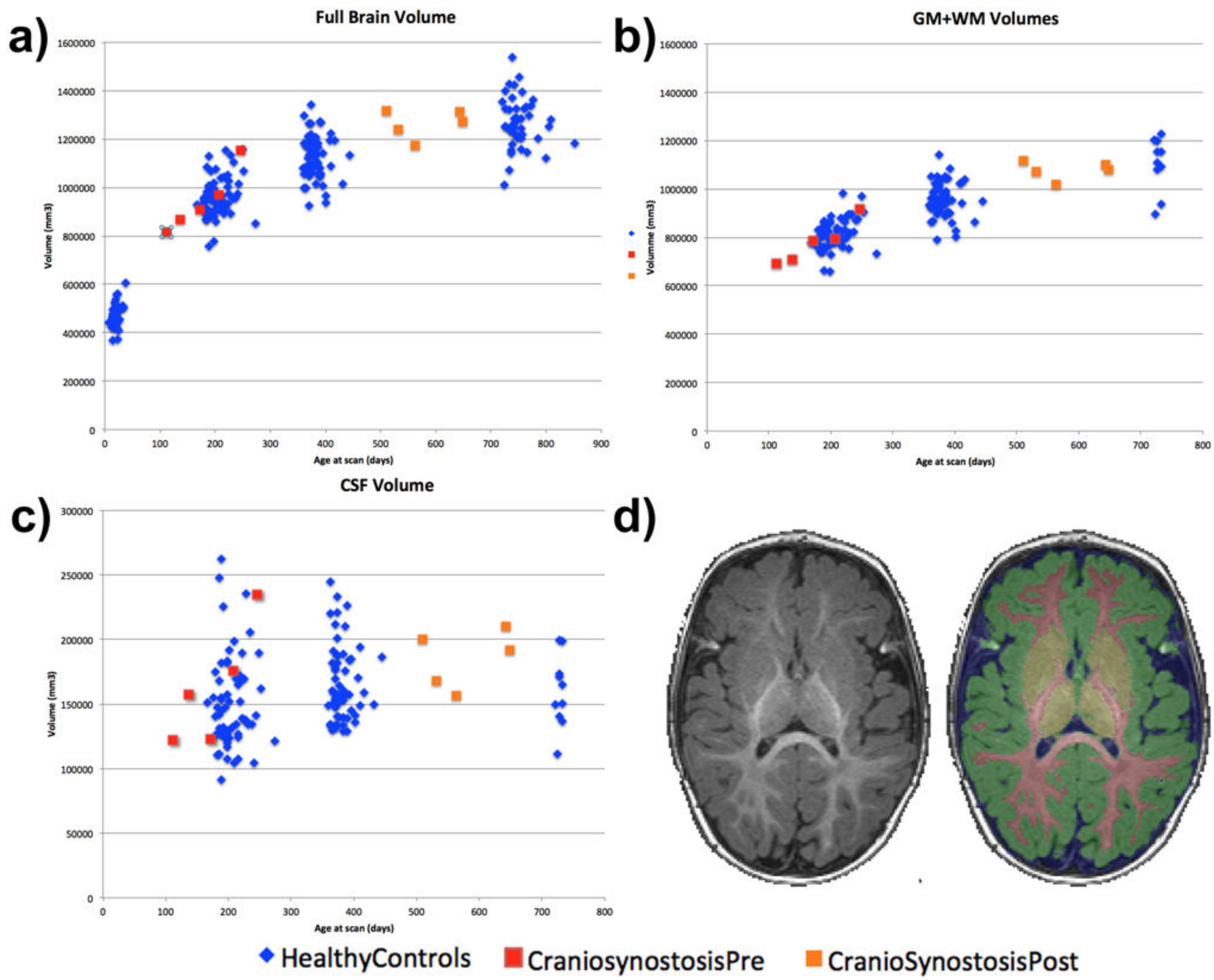

Figure 2.

Scatterplots for different imaging-derived volumetric data: a) ICV volume (non-regressed), b) WM + GM volume, c) CSF volume and d) MR T1-w image of a pre-surgical craniosynostosis (left) and label segmentation (right) displaying WM in red, GM in green and CSF in blue.

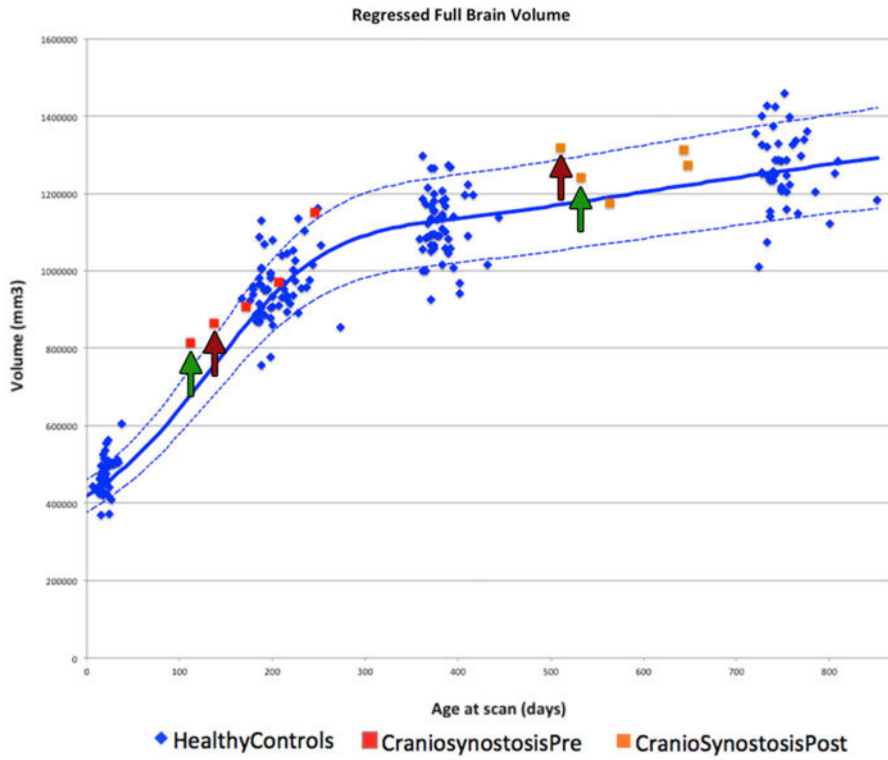

Figure 3.

Scatterplot for the ICV volumes obtained from the 4D model of normative evolution. Solid line blue line indicates the mean healthy atlas with one and minus standard deviations displayed in dashed blue. Red arrows indicate the pre- and post-surgical ICV measurements obtained from a sagittal craniosynostosis patient for which surgery did not normalize the volume, whereas green arrows indicate the pre- and post-surgical ICV measurements from a patient for which surgery did helped normalizing ICV.

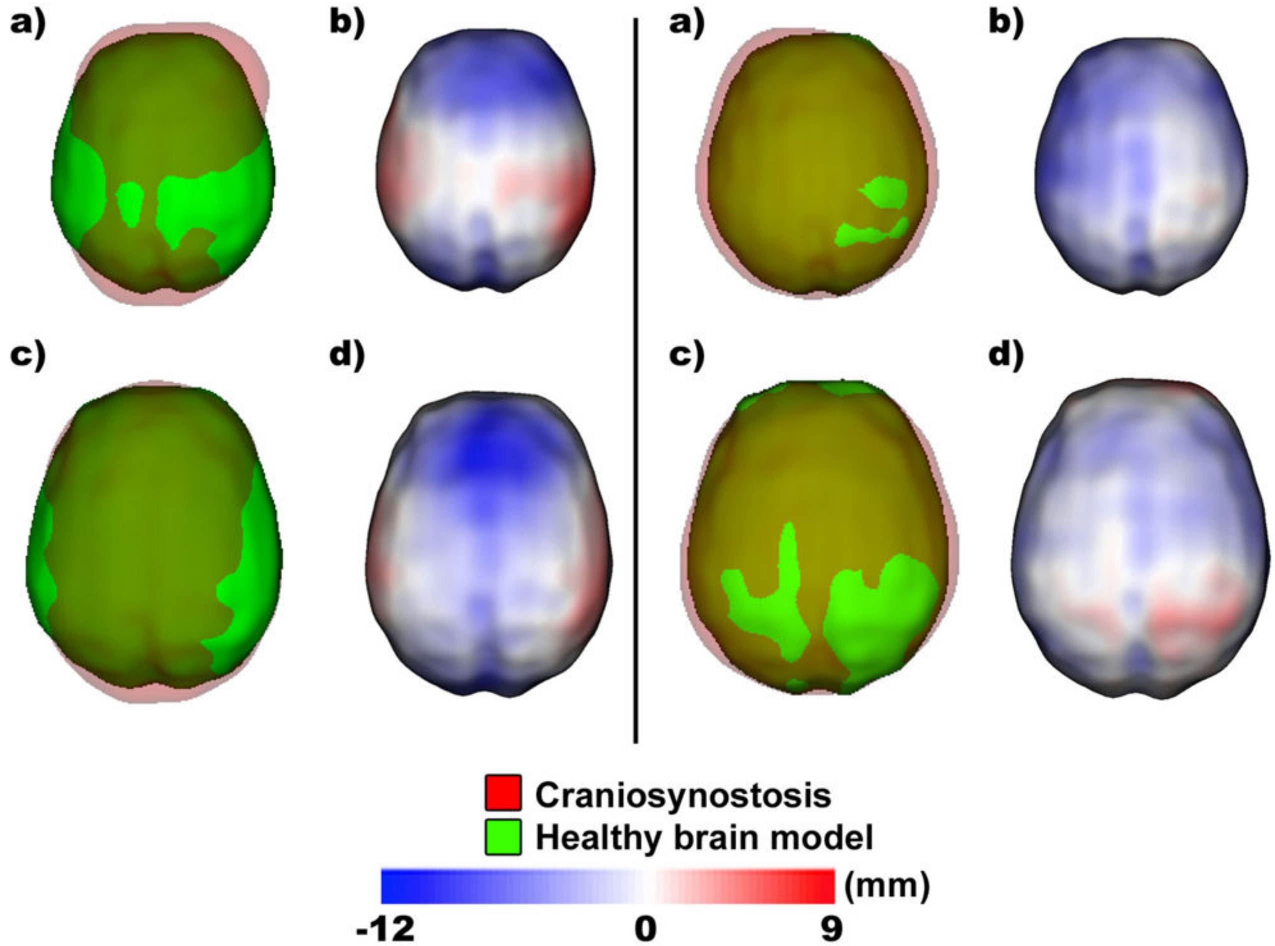

Figure 4.

Example of shape analysis for a patient for which ICV did not normalize after surgery (on the left) and another patient for which ICV did normalize after surgery (on the right). a) pre-surgical and c) post-surgical semitransparent overlays between (green) age matched normal brain shape and (red) brain shape for the patient. b) pre-surgical and d) post-surgical shape analysis measurements illustrating the magnitude and the direction (compression – red, expansion – blue) of shape changes.